⌘ Author's Choice

An Unbiased Proteomic Screen Reveals Caspase Cleavage Is Positively and Negatively Regulated by Substrate Phosphorylation*[S]

Jacob P. Turowec‡, Stephanie A. Zukowski‡, James D. R. Knight§, David M. Smalley¶, Lee M. Graves¶, Gary L. Johnson¶, Shawn S. C. Li‡, Gilles A. Lajoie‡, and David W. Litchfield‡

Post-translational modifications of proteins regulate diverse cellular functions, with mounting evidence suggesting that hierarchical cross-talk between distinct modifications may fine-tune cellular responses. For example, in apoptosis, caspases promote cell death via cleavage of key structural and enzymatic proteins that in some instances is inhibited by phosphorylation near the scissile bond. In this study, we systematically investigated how protein phosphorylation affects susceptibility to caspase cleavage using an N-terminomic strategy, namely, a modified terminal amino isotopic labeling of substrates (TAILS) workflow, to identify proteins for which caspase-catalyzed cleavage is modulated by phosphatase treatment. We validated the effects of phosphorylation on three of the identified proteins and found that Yap1 and Golgin-160 exhibit decreased cleavage when phosphorylated, whereas cleavage of MST3 was promoted by phosphorylation. Furthermore, using synthetic peptides we systematically examined the influence of phosphoserine throughout the entirety of caspase-3, -7, and -8 recognition motifs and observed a general inhibitory effect of phosphorylation even at residues considered outside the classical consensus motif. Overall, our work demonstrates a role for phosphorylation in controlling caspase-mediated cleavage and shows that N-terminomic strategies can be tailored to study cross-talk between phosphorylation and proteolysis. ***Molecular & Cellular Proteomics 13: 10.1074/mcp.M113.037374, 1184–1197, 2014.***

From the ‡Department of Biochemistry, Schulich School of Medicine and Dentistry, Western University, London, Ontario N6A 5C1, Canada; §Samuel Lunenfeld Research Institute, Mount Sinai Hospital, Toronto, Ontario M5G 1X5, Canada; ¶Department of Pharmacology, The University of North Carolina at Chapel Hill, Chapel Hill, North Carolina 27514

⌘ *Author's Choice*—Final version full access.

Received December 23, 2013, and in revised form, February 14, 2014

Published, MCP Papers in Press, February 20, 2014, DOI 10.1074/mcp.M113.037374

Author contributions: J.P.T., S.A.Z., L.M.G., G.L.J., S.S.L., G.A.L., and D.W.L. designed research; J.P.T., S.A.Z., and D.M.S. performed research; J.P.T., J.D.K., D.M.S., L.M.G., G.L.J., S.S.L., and G.A.L. contributed new reagents or analytic tools; J.P.T., S.A.Z., J.D.K., D.M.S., G.A.L., and D.W.L. analyzed data; J.P.T., S.A.Z., J.D.K., L.M.G., G.L.J., and D.W.L. wrote the paper.

Apoptosis is a cell death program integral to various biological processes such as tissue homeostasis and development (1). The ability of cancer cells to evade apoptosis is considered a driving feature that imparts a selective cellular advantage allowing cells to persist inappropriately (2). A major component of apoptotic evasion in cancer arises from the misregulation of two enzyme classes, protein kinases and caspases. Kinases transfer the γ-phosphate from ATP to proteins to alter substrate function, and caspases act as executioners of the apoptotic program by facilitating the demolition of cellular constituents by cleaving key structural and enzymatic proteins (3, 4). Attenuation of caspase activity arising through kinase-mediated post-translational modifications or genetic mutations or deletions can contribute to malignant phenotypes by blocking apoptotic progression (5, 6).

Interestingly, numerous examples have implicated cross-talk between caspases and kinases as a major apoptotic regulatory mechanism, and anecdotal examples have been identified in which phosphorylation at P4, P2, and P1′ (see Fig. 1*A* for cleavage site nomenclature) has been shown to block cleavage and affect cellular phenotypes (6–12). Accordingly, phosphorylation-dependent regulation of caspase-mediated cleavage has been hypothesized as a global regulator of apoptotic progression, especially in the context of cancer, where hyperactive, oncogenic kinases may act to increase phosphosite occupancy within caspase cleavage motifs (7). Indeed, we previously tested this hypothesis using predictive peptide match programs and identified CK2 phosphorylation sites on caspase-3 that regulated its activation by caspase-8 and -9 (13).

To build on our predictive strategy, we devised an unbiased, proteomic methodology to identify novel proteins for which phosphorylation regulates cleavage via caspases. We measured the caspase degradome in the context of a native phosphoproteome and compared it to the caspase degradome generated from lysates formerly dephosphorylated with λ bacteriophage phosphatase. To identify these events, we utilized the N-terminomic workflow TAILS[1] (terminal amino

[1] The abbreviations used are: TAILS, terminal amino isotopic labeling of substrates; caspase, cysteine-dependent aspartate-directed protease; λ phosphatase, phosphatase derived from bacteriophage λ; DNP, 2,4-dinitrophenol; PARP1, poly(ADP-ribose) polymerase.

isotopic labeling of substrates) (14). Comparative analysis of the caspase degradomes from phosphorylated and dephosphorylated lysates revealed Yap1 and Golgin-160 as caspase substrates negatively regulated by phosphorylation.

Surprisingly, we also identified a number of caspase substrates for which cleavage is promoted by phosphorylation, and during the course of our study, Dix *et al.* (15) demonstrated that phosphorylation at P3 can promote the cleavage of caspase peptide substrates. Our proteomic screen highlighted MST3 as a caspase substrate positively regulated by phosphorylation; however, in contrast to results obtained for MST3 protein in lysates, phosphorylation exerted a negative influence on the cleavage of an MST3 peptide, as was the case for other peptides modeled after Yap1 and Golgin-160. Collectively, these data suggest that although inhibitory effects of phosphorylation can arise through phosphorylation of residues proximal to the cleavage site, the positive effect of phosphorylation may stem from determinants other than those near the scissile bond. Subsequently, to test the effect of phosphorylation throughout the entirety of the caspase motif, we systematically walked phosphoserine through the length of model caspase-3, -7, and -8 substrate peptides and found that phosphorylation was generally inhibitory to caspase cleavage. Again, these observations suggest that positive effects of phosphorylation on the caspase cleavage of proteins observed in lysates likely arise through modulated ternary protein structure. Overall, our studies demonstrate that N-terminomics approaches can be tailored to identify novel, hierarchical events controlling the cleavage of caspase substrates.

EXPERIMENTAL PROCEDURES

Caspase Degradome Preparation—HeLa cells were cultured in Dulbecco's modified Eagle's medium containing 10% fetal bovine serum, penicillin (100 U/ml), and streptomycin (100 mg/ml). Cells were treated for 45 min with 1 μM okadaic acid (Bioshop Canada Inc., Burlington, Ontario, Canada) and then lysed in caspase assay buffer (0.1% CHAPS, 20 mM PIPES (pH 7.4), 100 mM NaCl) and protease and phosphatase inhibitors (leupeptin (10 μg/ml), 0.1 mM phenylmethylsulfonyl fluoride (PMSF), pepstatin A (10 μg/ml), aprotinin (5 μg/ml), 50 mM NaF, 1 μM microcystin, and 1 mM sodium orthovanadate). Cells were lysed by sonication with two pulses of 5 s each, and the samples were subsequently cleared by ultracentrifugation at 13,000 $\times$ *g* if being used for Western blot analysis or 140,000 $\times$ *g* if being used for proteomic analysis. Lysates were then exchanged into 100 mM HEPES (pH 7.0) 3$\times$ using 3 K cut-off buffer exchange filters (Amicon, Billerica, MA) to remove phosphatase inhibitors prior to λ phosphatase treatment and small-molecule primary amines to permit complete dimethyl labeling of primary amines on proteins. The protein concentration was determined by using the Bradford assay. After buffer exchange, the sample was split in two, diluted in 10$\times$ phosphatase buffer (NEB) and 5$\times$ caspase buffer (see above for the 1$\times$ recipe), and then treated with or without λ phosphatase (10 U NEB λ phosphatase per microgram of lysate) for 1 h at 37 °C. Next, lysates were treated with 50, 500, or 5000 nM of caspase-3 and caspase-7 for 1 h at 37 °C, and the reaction was terminated by the addition of 6 μM irreversible caspase inhibitor z-VAD-fmk (Sigma). Caspase concentrations of 50 and 500 nM were used in TAILS experiments. For validation studies employing Western blot, we also included a higher caspase concentration (5000 nM) to ensure that caspase concentrations were not limiting and to stringently assess the protective effect of phosphorylation. Finally, samples previously left phosphorylated were treated with λ phosphatase as described above, and either samples were further processed using TAILS for proteomic analysis or 2$\times$ Laemmli buffer was added for Western blotting.

Sample Preparation Using TAILS—TAILS was performed largely as described previously (16). Briefly, caspase degradomes were diluted 1:1 in 8 M guanidine hydrochloride. Cysteine residues were reduced by 5 mM DTT, incubated at 65 °C for 1 h, and then alkylated by iodoacetamide treatment for 2 h at room temperature in the dark. After excess iodoacetamide had been quenched with DTT, the pH was adjusted to 6.5 using 0.5 N HCl to prepare for the dimethyl labeling of primary amines. Primary amino groups were dimethylated by the addition of 20 mM $NaBH_3CN$ and 40 mM $^{12}CH_2$-formaldehyde (light) (Sigma) or $^{13}CD_2$-formaldehyde (heavy) by reaction at 37 °C overnight, followed by quenching with 100 mM Tris (pH 6.8) for 4 h. Samples were mixed at this point, and proteins were precipitated with cold methanol and acetone (8:1), washed three times with methanol to remove excess label and amines, resuspended in 8 M guanidine hydrochloride, and diluted 8-fold in 1 M HEPES (pH 8.0). Trypsin (Promega, Madison, WI) was added (1:100 trypsin:lysate (w/w)) and samples were incubated overnight at 37 °C, with incubation followed by a fresh trypsin addition (1:200) for another 4 h. Finally, internal tryptic peptides were reacted with HPG-ALDII polymer (Flintbox, Pittsburg, PA) to negatively select for protein N termini and caspase-generated dimethylated neo-N termini. Here, 2 mg of polymer and 20 mM $NaBH_3CN$ were added to 1 mg of lysate, the pH was adjusted to 6.5 with HCl, and the reaction incubated at 37 °C overnight. After quenching with 100 mM Tris (pH 6.8), negative selection of N termini was performed by filtering the polymer (~80 kDa) with a 10-kDa-cutoff Microcon spin-filter as per the manufacturer's instructions. We cleaned up the N terminome containing flow-through on a C_{18} light Waters Sep-Pak by acidifying the sample in 0.1% formic acid, applying it to the column, washing with 0.1% formic acid, and eluting in 80% acetonitrile/0.5% formic acid. Samples were then vacuum centrifuged and stored at −20 °C until mass spectrometry analysis.

Peptide Identification Using Mass Spectrometry—The peptides were resuspended in 2% acetonitrile/0.1% formic acid/97.9% water and loaded onto a 2 cm long $\times$ 360 μm outer diameter $\times$ 100 μm inner diameter microcapillary fused silica precolumn packed with Magic 5-μm C18AQ resin (Michrom Biosciences, Inc., Auburn, CA). After sample loading, the precolumn was washed with 95% solvent A (0.1% formic acid in water)/5% solvent B (0.1% formic acid in acetonitrile) for 20 min at a flow rate of 2 μl/min. The precolumn was then connected to a 360 μm outer diameter $\times$ 75 μm inner diameter analytical column packed with 14 cm of 5-μm C18 resin constructed with an integrated electrospray emitter tip. The peptides were eluted at a flow rate of 250 nL/min by increasing the percentage of solvent B to 40% with a Nano-Acquity HPLC solvent delivery system (Waters Corp., Mississauga, Ontario, Canada). The LC system was directly connected through an electrospray ionization source interfaced to an LTQ Orbitrap Velos ion trap mass spectrometer (Thermo Electron Corp., Waltham, MA). The mass spectrometer was controlled by Xcalibur software (Thermo, v. 2.1.0.1140) and operated in the data-dependent mode in which the initial MS scan recorded the mass-to-charge ratios (*m/z*) of ions over the range of 400–2000. The 10 most abundant ions were automatically selected for subsequent collision-activated dissociation in ion trap mode. Each sample was run in duplicate. Raw files were searched and quantified using Maxquant (17) version 1.2.2.5 using the UniProt database (84,909 sequences, November 20, 2012). Searches included cysteine residues as a fixed modification of +57.0215 Da, oxidized methionine

residues as a variable modification of +15.9949 Da, and deamidated asparagine and glutamine residues as a variable modification of +0.9840. Light and heavy dimethylation of peptide amino termini and lysine residues were set as variable modifications of +28.0313 Da and +34.0631 Da, respectively. Peptides were queried using Asp-C (caspase cleaves only after Asp residues) and Arg-C (trypsin cannot cut after dimethylated lysine) cleavage constraints with a maximum of two missed cleavage sites. The mass tolerances were 6 ppm for parent masses and 0.6 Da for fragment masses. The peptide false discovery rate was set at 0.01. Only peptides identified in at least two runs were used, and peak ratios were averaged by taking the geometric mean of the heavy:light ratio. Technical duplicates of three experiments were performed. Protein N-terminal peptide and P1 Asp peptide ratios were normalized by dividing all ratios by the average ratio of the protein N-terminal peptides. The weblogo of P1 Asp peptides was determined as previously described (18).

Western Blotting—Samples were separated on SDS-PAGE gels and transferred to PVDF membrane using standard procedures. Membranes were blocked with 5% BSA/TBS–Tween 20 and probed overnight with primary antibodies in 1% BSA/TBS–Tween 20. PKCδ, MST1, MST3, Yap1, and Golgin-160 antibodies were all purchased from Abcam, Toronto, Ontario, Canada. Presenilin-1 antibodies were from Novus Biologicals, Littleton, CO, phospho-Histone H2B was from Cellular Signaling Technology, Danvers, MA, and phospho-EEF1D and phospho-EEF1B were made as previously described (19). Secondary antibodies conjugated with fluorogenic 680 or 800 dyes were purchased from Li-COR Biosciences, and blots were imaged using a Li-COR Odyssey imager, Lincoln, NE.

Apoptotic Induction of HeLa Cells—Cells were treated with 1 μM staurosporine (LC Laboratories, Woburn, MA) and 500 nM okadaic (Bioshop, Burlington, Ontario Canada), with both drugs or with a carrier (dimethyl sulfoxide) control for 3 h. Cells were collected and lysed in Nonidet P-40 alternative lysis buffer (1% Nonidet P-40 alternative, 150 mM NaCl, 50 mM Tris (pH 7.5), leupeptin (10 μg/ml), 0.1 mM PMSF, pepstatin A (10 μg/ml), aprotinin (5 μg/ml), and 1 μM zVAD-fmk (Sigma)). After brief sonication and clearance of insoluble material by centrifugation (13,000 × *g* for 15 min at 4 °C), the protein concentration was assessed using a bicinchoninic acid assay (Thermo Scientific). Lysates were dephosphorylated as described above to reduce the differential migration of phosphorylated proteins, thereby simplifying Western blot analysis. Approximately 20 μg of lysates were then separated on SDS-PAGE gels and blotted as described above.

Peptides—PARP1 and caspase-3 peptides were synthesized as previously described (13) via standard Fmoc-based peptide chemistry with an Automated Multiple Peptide Synthesizer (Intavis, Cologne, Germany). Fmoc-Lys(dinitrophenol)-OH (Bachem, Torrance, CA) was attached to the C terminus of each peptide, and peptides were capped with Fmoc-Trp-OH and biotin at the N terminus. Phosphorylated peptides were generated with Fmoc-Ser [Ser[PO(OBzl)-OH]-OH (AnaSpec, Fremont, CA). Peptides were resuspended in 250 mM HEPES (pH 7.5) and the pH was adjusted to 7.5 with NaOH. The peptide concentration was determined by OD 355, and identity was verified via MALDI-TOF. Peptide series for MST3, Yap1, and Golgin-160 were synthesized by ChinaPeptides, Shanghai, China. Quality control documents for HPLC chromatography and mass spectrometry were provided as verification of purity (>95%) and peptide identity, respectively.

Caspase Assays—Recombinant caspase-3 (Addgene plasmid number 11821 (20)), caspase-7 (Addgene plasmid number 11825 (20)), and caspase-8 (Addgene plasmid number 11827 (20)) were purified and their activity was assessed via active site titration as described previously (21). Peptides used as caspase substrates were synthesized with a FRET pair of tryptophan and lysine-DNP at either terminus. Quenching of tryptophan fluorescence by DNP is relieved by caspase cleavage, allowing one to determine caspase cleavage by monitoring tryptophan fluorescence at 355 nm. Caspase-3 assays were performed with 200 nM (PARP1), 800 nM (Yap1, Golgin-160), or 1.2 μM (MST3) caspase and 100 μM peptide at 37 °C in 20 mM PIPES (pH 7.4), 100 mM NaCl, 5% sucrose, 0.1% CHAPS (w/v), and 5 mM DTT for 15 min. Caspase-7 assays were performed in the same buffer, but with 200 nM (Golgin-160), 500 nM (Golgin-160), 600 nM (PARP1), 1 μM (MST3), or 2.5 μM (Yap1) caspase. Caspase-8 reactions were performed with 100 nM caspase-8 in 1 M sodium citrate and 35 mM NaH_2PO_4/Na_2HPO_4 (pH 7.4) at 37 °C for 5 min. Dephosphorylation of peptides prior to caspase treatment was achieved using an excess of recombinant bacteriophage λ phosphatase in Protein MetalloPhosphatase buffer (NEB) with 1 mM $MnCl_2$ for 1 h at 37 °C. Caspase reactions were quenched by the addition of the irreversible caspase inhibitor z-VAD-fmk (Sigma), diluted 1 in 4 and emission read at 355 nm after excitation at 280 nm. Fluorescence was measured on a Horiba fluorolog-3 spectrofluorometer (supplemental Fig. S4*A*) or on a SpectraMax M5 fluorescence plate reader. Reactions were performed in quadruplicate, and analysis of variance and Tukey's test were used to compare the mean fluorescence of phosphorylated peptides with that of their unphosphorylated or phosphatase-treated counterparts.

RESULTS

Unbiased Proteomic Evaluation of Phosphorylation-dependent Regulation of Caspase-mediated Cleavage—In an effort to characterize the interplay between phosphorylation and caspase-mediated degradation, we applied a proteomics approach to identify phosphorylation-regulated caspase substrates. In our workflow, lysates from HeLa cells (treated with okadaic acid to preserve cellular phosphorylation) were treated with or without λ phosphatase followed by recombinant caspase (Fig. 1*B*). In order to maximize the number of substrates identified while minimizing the number of mass spectrometry runs, we added a mixture of two executioner caspases, caspase-3 and caspase-7, that are responsible for the majority of cleavage events in apoptosis and have almost identical consensus motifs (22, 23). Next, we utilized TAILS as a means for enriching the proteome for caspase substrates (14). Here, caspase-degraded proteomes are isotopically labeled at N-terminal residues and lysine residues with heavy (+34) or light (+28) formaldehyde. Trypsin digestion reveals internal peptide N termini whose amine groups are reactive against an aldehyde-coupled, high-molecular-weight resin, whereas the amine groups of protein N termini and caspase-generated N termini remain inert as a result of blockage by dimethylation. Filtering the lysate through a 10K cut-off membrane removes the reacted resin/internal tryptic peptide species, allowing for enrichment of the N-terminome in the flow-through. Performing LC-MS/MS analysis on an LTQ-Orbitrap identifies N termini, and from the differential dimethyl labeling, ion intensities from MS are used to produce a quantitative comparison between caspase degradomes from phosphorylated and dephosphorylated lysates. Importantly, after digestion with caspases, the phosphorylated lysate was treated with phosphatase. This allowed a direct quantitative comparison between caspase substrates that might have a phos-

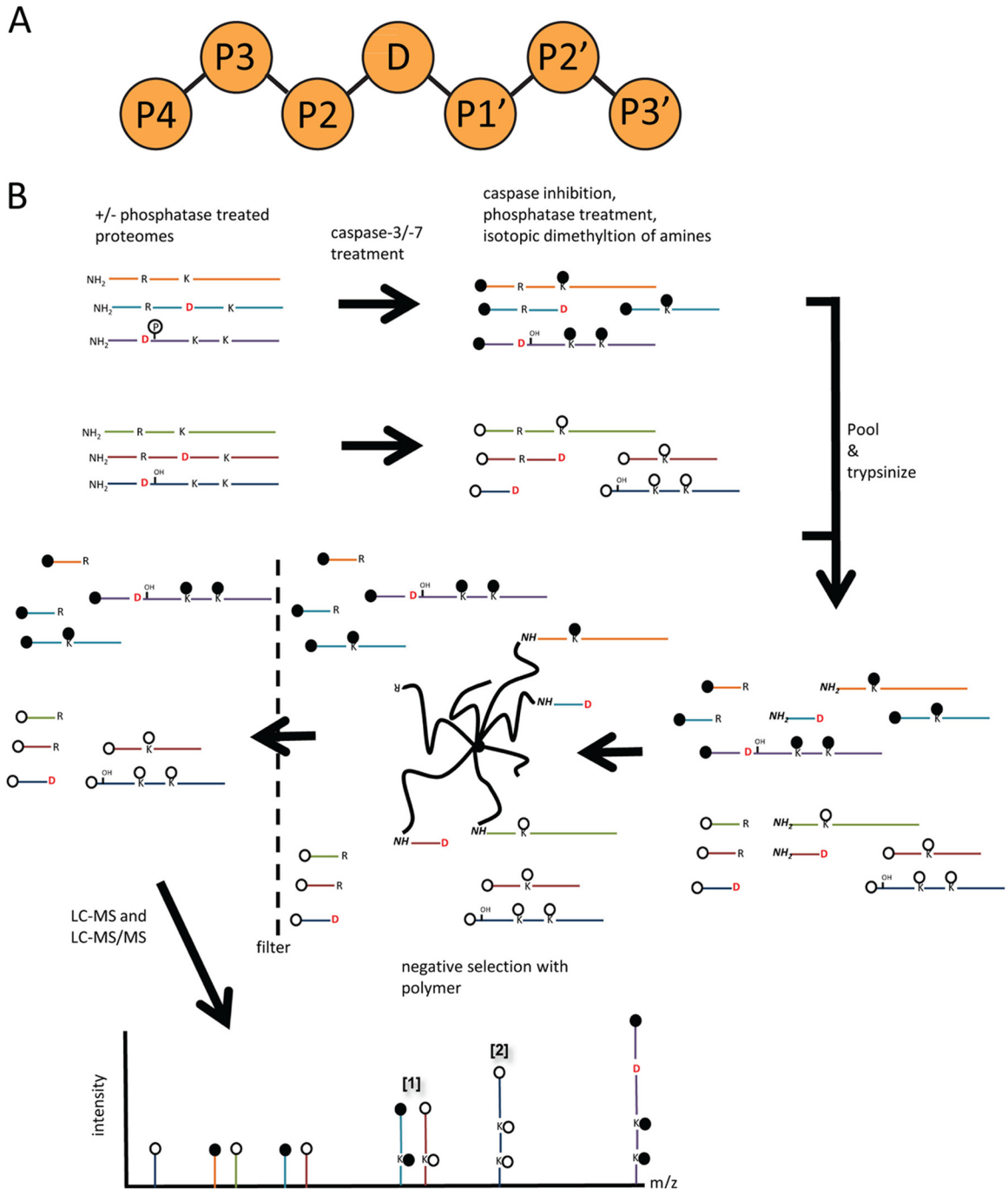

FIG. 1. **Workflow for the global, unbiased analysis of the integration of phosphorylation and caspase-mediated degradation.** *A*, illustration of the cleavage site nomenclature for proteases. Caspases cleave the scissile bond between a P1 aspartic acid and the P1′ residue. *B*, HeLa cell lysates were treated with or without λ phosphatase and subjected to caspase treatment followed by dephosphorylation of the sample previously left phosphorylated. Primary amines on protein N termini and lysine residues were dimethylated using heavy (+34, open circles) or light (+28, black circles) formaldehyde. Samples were pooled and trypsinized, which exposed an amine on the N terminus of the internal tryptic peptide. These peptides are captured through reaction with an ~80-kDa aldehyde-substituted polymer. Importantly, native protein N termini and neo-N termini generated by caspase cleavage are resistant to reaction with the polymer because their reactive amines have been blocked by dimethylation. Enrichment of the N-terminome then occurs via negative selection when the reacted polymer is filtered away using a 10-kDa cut-off spin column. LC-MS/MS analysis of isotopically dimethylated peptides then allows comparative analysis between caspase degradomes of phosphorylated and dephosphorylated lysates. Caspase substrates will be inferred through identification of those peptides with a P1 aspartic acid. In the event that there is no difference in caspase substrate proteolysis between phosphorylated and dephosphorylated samples, a peptide ratio of ~1:1 will be observed in MS1 [1]. Of interest are those peptide pairs that deviate from a 1:1 ratio [2].

phorylation site that, if occupied, would alter retention time or mass and undermine comparative analyses.

Before analyzing proteomic samples via mass spectrometry, we first tested for the efficient dephosphorylation of cell extracts and the presence of cleaved caspase substrates. Samples were analyzed at different points throughout the workflow (supplemental Fig. S1) for EEF1D and EEF1B phosphorylation and caspase cleavage of the previously identified substrate MST1 (24). λ phosphatase treatment resulted in efficient dephosphorylation of phospho-EEF1D and phospho-EEF1B, two abundant phosphorylated proteins with near stoichiometric phosphorylation (supplemental Fig. S1*A*, lanes 1 and 2) (19). Next these samples were treated with 50 or 500 nM caspase-3 and caspase-7, which resulted in a dose-dependent decrease in full-length MST1 (supplemental Fig. S1*A*, lanes 3–6). Finally, the addition of λ phosphatase to previously phosphorylated lysate abolished phospho-EEF1D and phospho-EEF1B antibody reactivity (supplemental Fig. S1*A*, lanes 3 and 5). Further validating the efficiency of our enzyme treatments, we found that lysate phosphatase assays abolished the reactivity of phospho-H2B antibodies when using extracts generated from nocodazole arrested cells and increased migration for total Presenilin-1 levels, again indicative of complete dephosphorylation (supplemental Fig. S1*B*). We also tested PKCδ, another known caspase substrate (25), for cleavage in lysates treated with a gradient of caspase-3 and caspase-7 concentrations (supplemental Fig. S1*C*). Proteolysis was again dose dependent and occurred with levels of caspases used previously in lysate cleavage assays (26).

Confident in our enzyme treatments of cell lysates, we generated TAILS samples from extracts treated with or without λ phosphatase and 50 or 500 nM caspase-3 and caspase-7. We identified and quantified 57 peptides with a P1 Asp, suggestive of caspase cleavage (see supplemental Table S1 and supplemental Fig. S2 for MS2 spectra). Only peptides identified in at least two replicates (either biological or technical) were considered hits. WebLogo analysis (18) of P1 Asp peptides generated a motif consistent with the consensus previously ascribed to caspase-3 and caspase-7 (DEVD, Fig. 2*A*) (23). Importantly, N-terminomic analysis of untreated Jurkat cells performed by Mahrus *et al.* (27) revealed that less than 5% of protein N termini contain a P1 Asp, reinforcing the conclusion that the majority of the P1 Asp peptides we identified were caspase substrates. As well, when our P1 Asp dataset was compared with the DegraBase repository of apoptotic N termini, we found that there was a 42% overlap, further substantiating the finding of *bona fide* caspase substrates in our data (supplemental Table S1) (28). Analysis of the $\log_2$ values of cleavage ratios comparing phosphatase treatment to control revealed a shift toward more cleavage in the control samples, perhaps indicating a general positive influence of phosphorylation on caspase cleavage at the proteome level (Figs. 2*B* and 2*C*). This skew was likely not due to labeling or sample bias, as P1 Asp quantitative data were normalized to the quantified protein N termini isolated using TAILS (see supplemental Table S2 and supplemental Fig. S3 for MS2 spectra), which should not change as a result of caspase treatment. In Fig. 2, we report the Gene Ontology of all identified caspase substrates (Fig. 2*D*) and of those positively regulated by phosphorylation (Fig. 2*E*); we found that a number of biological processes were represented. These observations are consistent with the broad effects of caspase during the progression of apoptosis.

To validate the quantitative data returned from TAILS analysis, we repeated lysate dephosphorylation/caspase experiments and probed for candidates using Western blotting. We focused on substrates with consistent changes in cleavage across multiple replicates and on those either previously identified as caspase substrates or whose cleavage site matched the caspase-3 and caspase-7 consensus motif. Using these criteria, we selected three candidates for validation: MST3, Yap1, and Golgin-160 (Fig. 3*A* and bars highlighted in red in Fig. 2*C*). MS/MS spectra for the identified P1 Asp peptides are shown in Figs. 3*B*, 3*C*, and 3*D*. The MST3 cleavage site ($AETD_{325}$) was reported previously (29), and we found that it was preferentially cleaved in phosphorylated lysates. Western blotting analysis revealed a modest but consistent change in the amount of full-length MST3 that differed between λ phosphatase–treated and untreated lysates (Fig. 3*E*, upper panel). In contrast, we found that Yap1 was preferentially cleaved when lysates were dephosphorylated. Though cleavage of Yap1 at $DEMD_{424}$ was not a previously known caspase site, the primary amino acid determinants do align with the caspase-3 and caspase-7 consensus motif, increasing our confidence that the site is a true positive. Furthermore, treating lysates with caspase-3 and caspase-7 resulted in a dose-dependent decrease of full-length Yap1, as well as the generation of smaller anti-Yap1 reactive bands (Fig. 3*E*, middle panel). Full-length Yap1 was also slightly more resistant to caspase cleavage when lysates were treated with λ phosphatase. Also, two degradation products persisted in the phosphorylated samples, which is also consistent with a protective role for phosphorylation (Fig. 3*E*, arrow and arrowhead). Lastly, we found that Golgin-160 (referred to as GOLGA3 in supplemental Table S1) was also cleaved less in phosphorylated lysates at $SEVD_{311}$, a site previously identified as targeted by caspase-3 and caspase-7 *in vitro* and in response to diverse apoptotic stimuli (30, 31). Repeating TAILS experiments and measuring cleavage by Western blotting, we obtained results that were again consistent with the data returned from TAILS (Fig. 3*E*, lower panel). Here, in the phosphatase-treated lysates, a more rapid conversion to the fully cleaved form was observed. In contrast, an intermediate, slower migrating cleavage fragment remained even at the highest dose of caspase-3 and caspase-7 (5 μM) in the phosphorylated lysates. Caspase-3 and caspase-7 can also cleave Golgin-160 at D_{59} and D_{139} (30), and so our blots were consistent with the model in which intermediate cleavage frag-

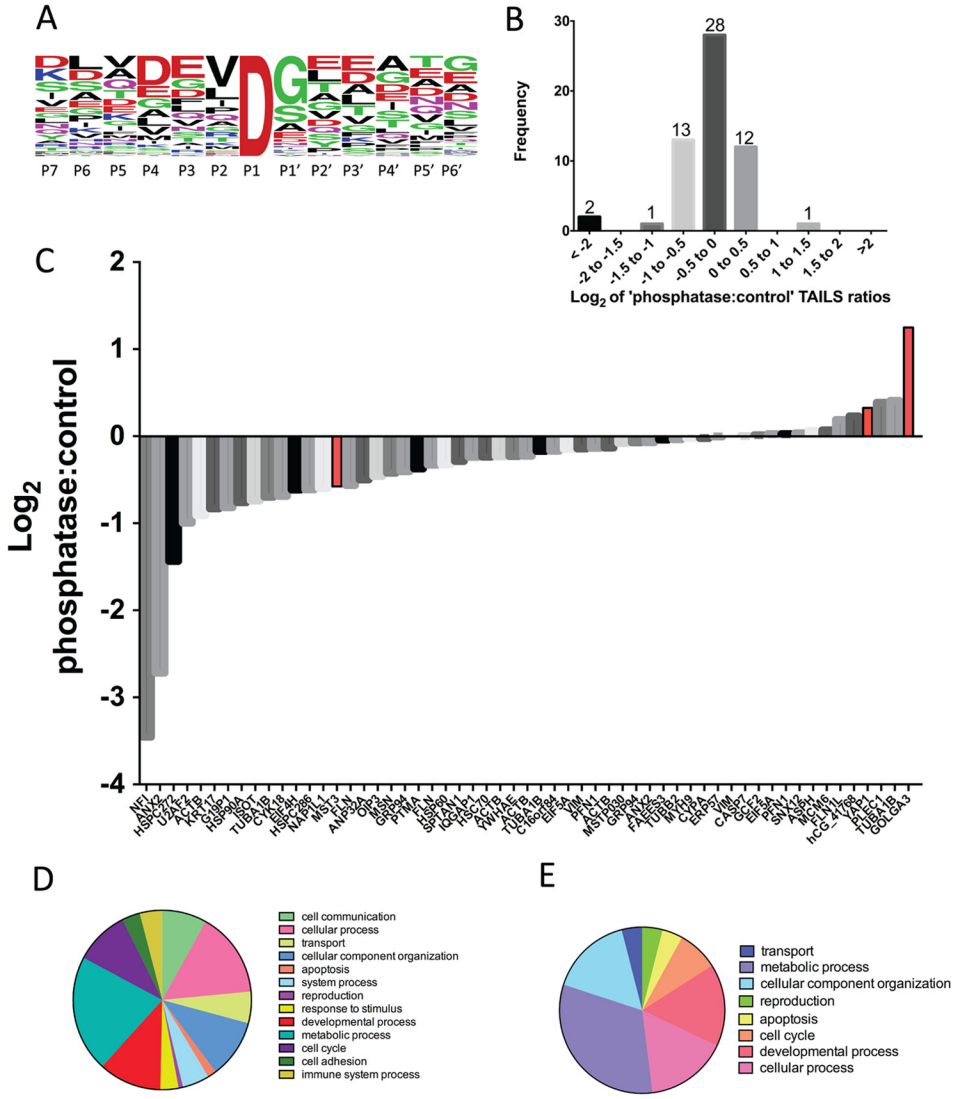

FIG. 2. **Summary of the peptides identified via TAILS.** *A*, a WebLogo analysis (18) of the 57 peptides with P1 aspartic acid that were identified via TAILS. *B*, a $\log_2$ histogram of the quantified P1 Asp peptides was plotted to visualize the distribution of the effect of phosphorylation on caspase cleavage. The number of peptides in each group is indicated. *C*, a $\log_2$ mountain plot of the quantified P1 Asp peptides. MST3, Yap1, and Golgin-160 are highlighted in red. The peptides and their relative abundance are also presented in supplemental Table S1. *D*, *E*, Gene Ontology (GO) analysis was performed for all P1 Asp peptides (*D*) or those positively regulated by phosphorylation (*i.e.* substrates with more pronounced regulation than MST3; see red bar with $\log_2 < 0$ in *C*) (*E*) using PANTHER (45, 46).

ments of Golgin-160 have been processed at these other residues but phosphorylation blocked proteolysis at $SEVD_{311}$. Ultimately, these data highlight novel mechanisms regulating the susceptibility of MST3, Yap1, and Golgin-160 to caspase cleavage.

Considering the notion that misregulation of oncogenic protein kinases can impede the progression of apoptosis (6, 7), we were interested in understanding the physiological relevance of phosphorylation events that block caspase substrate cleavage. To test how Golgin-160 and Yap1 phosphorylation affects their cleavage in cells, we induced HeLa cells to undergo apoptosis in the presence or absence of the phosphatase inhibitor okadaic acid. Apoptotic induction resulted in considerable PARP1 cleavage, a *bona fide* marker of caspase-3, -6, and -7 activity (32), in cells treated with staurosporine alone and in combination with okadaic acid (Fig. 3*F*). Interestingly, combination treatments reduced full-length Yap1 processing and almost completely blocked Golgin-160 cleavage. Similarly, the appearance of degradation bands for these proteins was reduced when apoptotic cells were treated with okadaic acid. We cannot rule out that indirect effects of okadaic acid treatment modulate cleavage of these substrates, but the patterns are consistent with that seen *in vitro* and support a role for either active substrate dephosphorylation upon apoptotic induction or okadaic-acid-induced increases in the stoichiometry of phosphorylation.

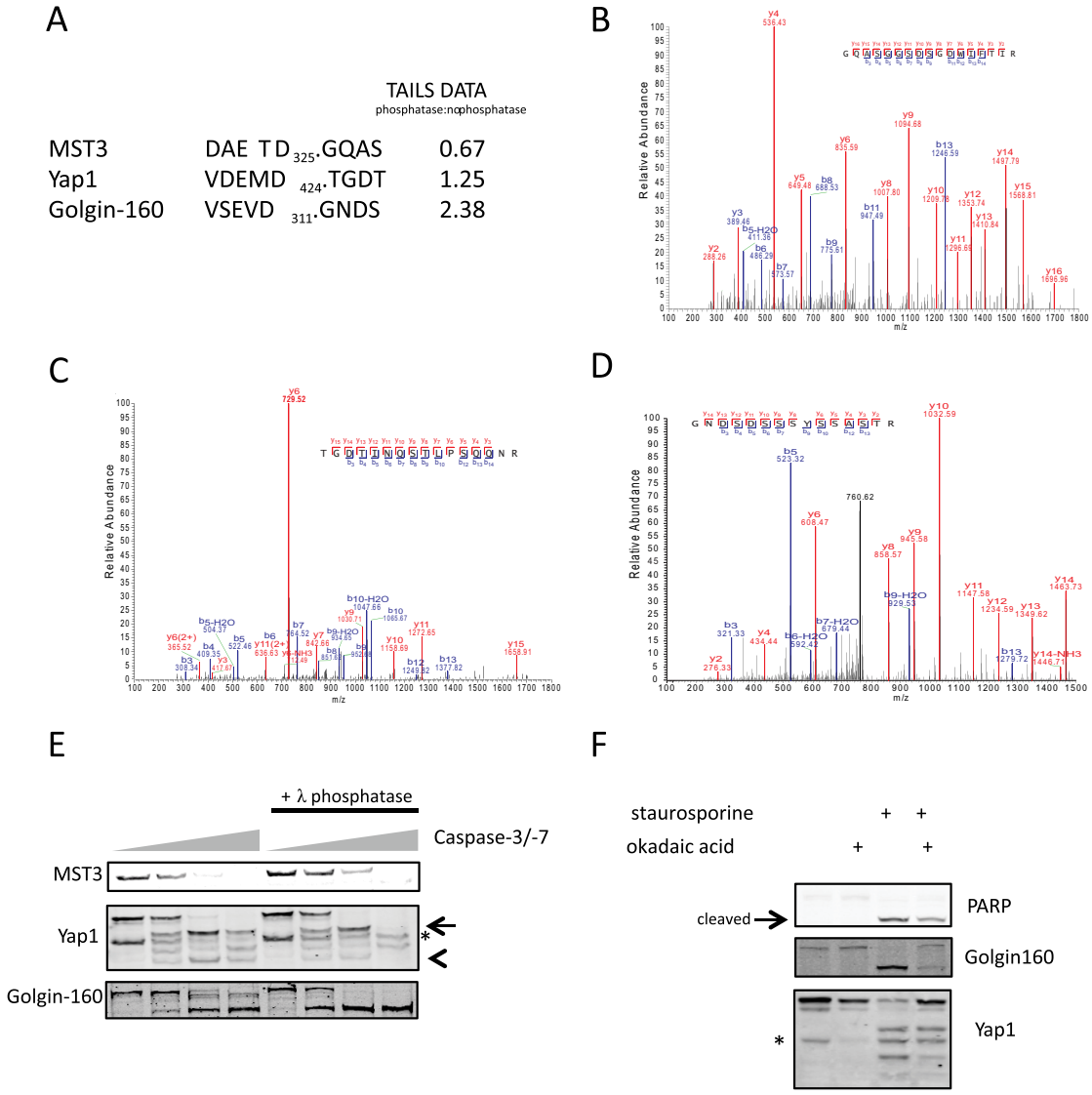

FIG. 3. **TAILS analysis revealed MST3, Golgin-160, and Yap1 as validated candidates in which cleavage is regulated by phosphorylation.** *A*, caspase recognition motif in MST3, Yap1, and Golgin-160. MS/MS analysis of MST3 (*B*), Yap1 (*C*), and Golgin-160 (*D*). *E*, HeLa lysates were treated identically to those samples prepared for N-terminomic analysis (as described in "Experimental Procedures"), except when they were utilized for Western blotting with antibodies directed against MST3, Yap1, or Golgin-160 as indicated. Caspase-3 and caspase-7 were used at concentrations of 0, 50, 500, and 5000 nM. The asterisk denotes a nonspecific band, and the arrow and arrowhead bands were differentially regulated by lysate dephosphorylation. *F*, HeLa cells were treated for 3 h with 1 μM staurosporine and/or 500 nM okadaic acid prior to lysis. Lysates were analyzed using immunoblots with the indicated antibodies. PARP1 cleavage was used as a control for caspase activation. The asterisk denotes a nonspecific band.

As a logical extension of the TAILS analysis, we were interested in systematically testing the effects of phosphorylation on cleavage using synthetic peptides modeled after caspase substrates identified by TAILS. For these studies, we generated a series of peptides to test whether phosphorylation within the caspase consensus motif was responsible for the observed differences in cleavage. Synthesized peptides were designed with the FRET pair of tryptophan and lysine-DNP at either terminus (supplemental Table S3). When the peptide is intact, emission by tryptophan at 355 nm after excitation at 280 nm is quenched by DNP, which absorbs at 355 nm. Following substrate cleavage, the release of tryptophan in close proximity to DNP abolishes quenching and permits monitoring of reaction rates by measuring tryptophan fluorescence at 355 nm. Indeed, reactions with control peptides that model the PARP1 cleavage site, which has previously been used as a peptide substrate for caspase-3 and caspase-7 (8, 13), maintained linearity through 15 min of reaction time and was not cleaved when the P1 residue was substituted to Ala (supplemental Fig. S4*A*). Similar results were seen for the caspase-8-mediated cleavage of caspase-3 model pep-

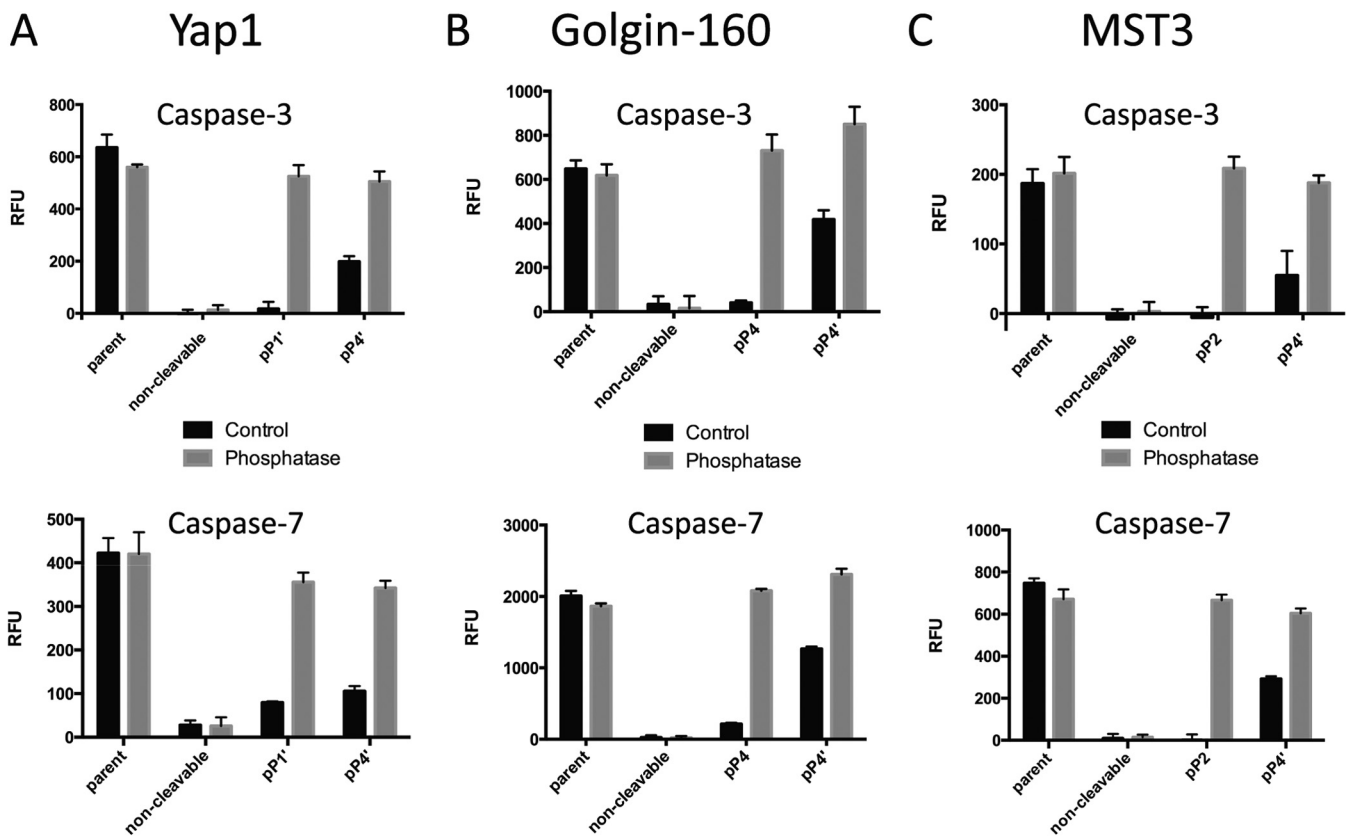

FIG. 4. **Caspase activities toward synthetic peptides modeled after substrates identified via TAILS.** Synthetic peptides or phosphopeptides modeled after Yap1 (*A*), Golgin-160 (*B*), or MST3 (*C*) were treated with or without λ phosphatase as indicated prior to incubation with caspase-3 or caspase-7. Fluorescence of an internally quenched tryptophan residue at 355 nm after excitation at 280 nm was measured to assess caspase cleavage of peptide substrates. Error bars represent the standard deviation of four reactions. Means for the caspase activities with phosphorylated peptides and their unphosphorylated counterparts were compared using analysis of variance and Tukey's test. Control *versus* phosphatase-treated pairs for phosphopeptides all had p values < 0.0001.

tides (supplemental Fig. S4*B*) and nonphosphorylated peptides modeled after MST3, Golgin-160, and Yap1 (data not shown), demonstrating the utility of this assay for monitoring caspase activity.

Synthetic peptides modeled after Yap1, Golgin-160, or MST3 were shown to be cleaved by either caspase-3 or caspase-7 (Fig. 4). In the case of Yap1 (Fig. 4*A*), phosphorylation of P1′ completely blocked cleavage. Interestingly, the phospho-P4′ peptide corresponding to Yap1 was also cleaved less efficiently than the nonphosphorylated parent peptide. Notably, this position is located a considerable distance from P4–P1′—the motif primarily responsible for directing caspase cleavage (23, 33)—and had not previously been shown to affect caspase cleavage. Phosphatase treatment confirmed the effects of phosphorylation, as dephosphorylation restored cleavage of both of the Yap1 phosphopeptides to the levels seen with nonphosphorylated parent peptide. Phosphorylation at P4, and to a lesser extent at P4′, also reduced cleavage of the Golgin-160 peptides (Fig. 4*B*). Again, phosphatase treatment of phosphopeptides restored caspase cleavage to the levels seen with the nonphosphorylated parent peptide. Results with Yap1 and Golgin-160 peptides corresponded well with results from TAILS experiments: dephosphorylation was shown to promote cleavage of both of these proteins, revealing a negative effect of phosphorylation on cleavage. The cleavage patterns exhibited by this series of peptides were shared between caspase-3 and caspase-7, a result that is supported by previous findings that note almost identical consensus motifs for these two caspases (23).

We were also interested in examining peptides modeled after proteins such as MST3 for which phosphorylation could have a positive effect on cleavage. In contrast to results seen with intact MST3 in lysates, where phosphorylation appeared to promote cleavage, phosphorylation at P2 completely abolished cleavage, and phosphorylation of P4′ also displayed an inhibitory effect. These data are discordant with the TAILS analysis, suggesting that these residues either (i) were not phosphorylated/dephosphorylated on full-length MST3 in our lysate assays or (ii) have context specific effects on cleavage that depend on the structure of the protein that are not represented in the primary sequence. To further explore the possibility that phosphorylation could promote cleavage, we also generated peptides modeled after NFI and ANX2, the two proteins that exhibited the most positive effects of phosphor-

ylation in lysates. We were unable to perform assays with the NFI peptide because of the low solubility of both nonphosphorylated and phosphorylated versions of these peptides. However, in the case of ANX2, the nonphosphorylated peptide had a low rate of cleavage that was not enhanced with the phosphorylated version of the peptide (data not shown). These data are consistent with the effects of phosphorylation residing in structural or distal, rather than proximal, primary sequence determinants.

Systematic Characterization of the Effect of Phosphoserine on Caspase Cleavage—By testing peptide models of candidate proteins identified in the TAILS analysis, we found that phosphorylation at four positions within P4–P4′ inhibited proteolysis. Interestingly, these data are somewhat at odds with our finding that phosphorylation appeared more likely to positively regulate the cleavage of proteins in lysates, and they suggest that in these instances phosphorylation events outside the caspase motif might be controlling proteolysis. The potential complexity of distal, structurally guided regulations coupled with the anecdotal examples here and elsewhere (8, 13) of caspase motif phosphorylation regulating proteolysis prompted us to systematically and rigorously define the determinant properties of phosphorylated residues throughout the caspase motif. To address this question, we designed three phospho-scanning model peptide series in which phosphoserine was positioned from P5–P4′ within the caspase-3/-7 model sequence and from P4–P3′ for the caspase-8 model sequence (supplemental Table S3). A broader series was used for caspase-3 and -7 because of the observation that primary amino acid specificity can extend beyond the canonical P4–P1′ residues for these caspases (34). Caspase-3 and -7 substrate series were modeled after Golgin-160 and the often used PARP1 sequence (8, 13), and a series based on the caspase-3 sequence served as a peptide substrate for the initiator caspase-8.

The phospho- and non-phosphopeptides for the Golgin-160 and PARP1 series produced essentially identical patterns for caspase-3 and caspase-7; this is perhaps not surprising given their extensive sequence and consensus motif similarity (Figs. 5*A* and 5*B*) (23, 35). Analyzing the unphosphorylated series revealed that the relative effect of serine throughout P5–P4′ was consistent with the literature. For instance, substituting serine for Asp at P4 decreased substrate conversion by a factor of 10 (data not shown) relative to the PARP1 model, but it became a measurable substrate at higher enzyme concentrations (see asterisk in Fig. 5*B*). Stennicke *et al.* (33) also observed a large decrease in K_{cat}/K_m when substituting aspartic acid at P4 to serine for caspase-3 and -7 peptide substrates. Similarly, substituting serine for glutamic acid at P3 decreased catalysis of Golgin-160 and PARP1, which is consistent with previous work (23). Whereas Stennicke *et al.* (33) reported no effect of serine at P1′, we observed a modest decrease in cleavage with serine at this position with both Golgin-160- and PARP1-derived peptides. Finally, we detected a reduction of cleavage when serine occupied P2 in the Golgin-160 peptide series, using either caspase, which is consistent with previous reports (23). Collectively, the analysis of serine throughout the consensus motif for caspase-3 and -7 model peptides demonstrated a strong correlation with the literature and validated our experimental system.

Golgin-160 and PARP1 phosphoserine peptides revealed an overall inhibitory effect of phosphorylation on proteolysis (Figs. 5*A* and 5*B*). Expectedly, phosphorylation at P2 (13) and P1′ (8) completely abolished cleavage. Phosphorylation at P3, which has previously been reported to have no effect on cleavage (8) as well as the capacity to promote cleavage in some instances (15), did not overtly alter proteolysis relative to the nonphosphorylated controls in our experiments. Our peptide series also investigated phosphorylated positions not previously assessed for their capacity to alter caspase cleavage. In this regard, phosphorylated P2′ almost completely abolished proteolysis. Phosphorylation at P3′ and P4′ had a modest inhibitory effect, as did phosphorylated P5, though the latter observation held only for the PARP1 model peptides. Overall, phosphorylated serine within four amino acids of the scissile bond decreased caspase-mediated cleavage, though phosphorylated P3 and P5 showed modest, model-specific effects.

We also extended our systematic analysis of the effect of caspase-motif phosphorylation on proteolysis to the initiator caspase-8. The effect of caspase-8 cleavage site phosphorylation showed trends similar to those of caspase-3 and caspase-7. Proteolysis was inhibited by phosphoserine at P4, P2, P1′, and P2′, whereas P3 was unaffected by phosphorylation (Fig. 6). To some degree, this latter result is in contrast to a recent report by Dix *et al.* (15), who found that phospho-P3 was exclusively a positive determinant for caspase-8 cleavage, but our findings are at least consistent in that inhibition was not observed when peptide substrates contained phosphorylated P3. Also, relative to caspase-3 and caspase-7, the effect of prime side phosphorylation on cleavage is less dramatic, as no significant difference between serine-P3′ and phosphoserine-P3′ was observed. Taken together with our N-terminomic data, the generally negative determinant properties of phosphoserine suggest that the phosphorylation-dependent promotion of proteolysis is controlled by factors outside of the primary amino acid sequence of the canonical caspase motif.

DISCUSSION

The convergence of caspase and kinase signaling has recently been described as a major mechanism in the regulation of apoptosis (6, 7). We utilized a TAILS N-terminomic strategy to monitor alterations in the caspase degradome of HeLa extracts by comparing the native phosphoproteome to lysates formerly dephosphorylated with λ phosphatase. Through this novel approach we identified caspase-mediated proteolytic

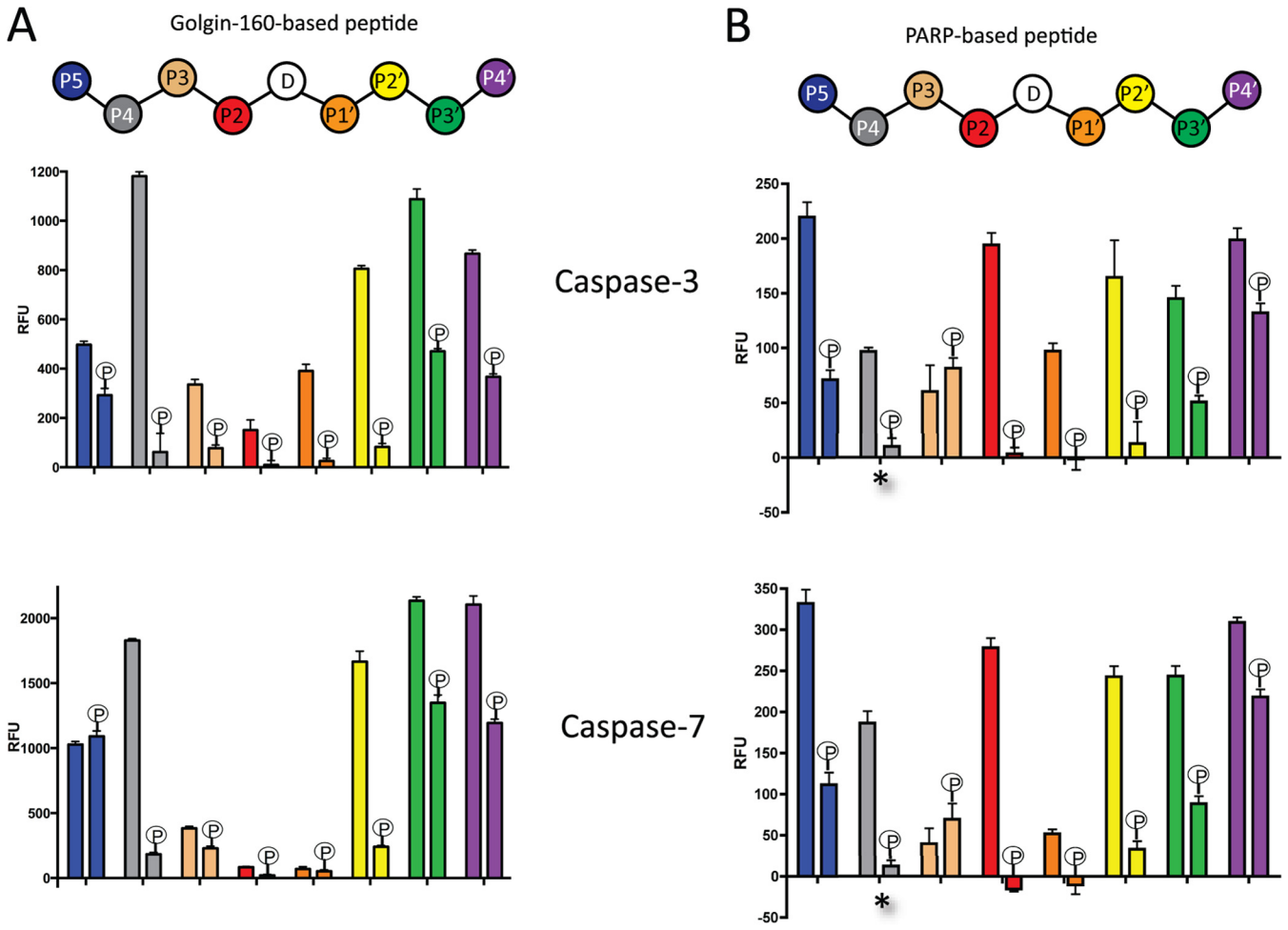

FIG. 5. **Relative activities of caspase-3 and caspase-7 with model and phosphopeptides containing serine residues positioned within the P5–P4′ consensus motif for caspase cleavage.** Caspase cleavage of peptide substrates was measured using fluorescence of an internally quenched tryptophan residue at 355 nm after excitation at 280 nm. Peptides or phosphopeptides modeled after Golgin-160 (*A*) and PARP1 (*B*) were assayed with caspase-3 or caspase-7 for 10 min at 37 °C and stopped by an excess of the irreversible caspase inhibitor zVAD-fmk. Error bars represent the standard deviation of four reactions. *A*, means of the caspase activities toward phosphorylated peptides and their nonphosphorylated counterparts were compared using analysis of variance and Tukey's test. For caspase-3, P4, P3, P1′, P2′, P3′, and P4′ phosphopeptide *versus* nonphosphorylated peptide pairs had p values < 0.0001, whereas all other pairs had a p value > 0.05. For caspase-7, P4, P3, P2′, P3′, and P4′ phosphopeptide *versus* nonphosphorylated peptide pairs had p values < 0.0001, whereas all other pairs had a p value > 0.05. *B*, cleavage of P4 peptides, in which serine or phosphoserine was substituted for aspartic acid, was not measurable at 200 nM of caspase-3 or 600 nM of caspase-7, so caspase concentrations were increased 5-fold (*). Error bars represent the standard deviation of four reactions. All pairs had p values < 0.0001, except for the P3 pair, which had a p value > 0.05.

events that were both positively and negatively regulated by phosphorylation. We identified and validated three proteins from our screen; Yap1 and Golgin-160 were degraded less when phosphorylated, whereas phosphorylation promoted cleavage of MST3. Approximately one in three identified caspase substrates exhibited an effect of phosphorylation on cleavage (based on proteins for which negative effects of phosphorylation were equal to or greater than that of Yap1 or positive effects of phosphorylation were equal to or greater than that of MST3). In accordance with the work of Dix *et al.* (15), our data suggest that the majority of proteins for which phosphorylation has an effect on cleavage undergo more extensive cleavage when phosphorylated. In fact, our TAILS analysis revealed that proteins in which phosphorylation appeared to promote cleavage outnumbered proteins in which phosphorylation prevented cleavage by more than 3-fold (15 proteins with more cleavage than MST3 in phosphorylated lysates *versus* 4 proteins with less cleavage than Yap1 in phosphorylated lysates). Overall, these data demonstrate the potential for widespread influence of phosphorylation on caspase cleavage.

One benefit of our experimental design was that it enabled us to monitor the effects of phosphorylation on cleavage irrespective of its distance from the scissile bond—an important consideration, as there is no way to predict how phosphorylation sites outside the caspase motif might affect the

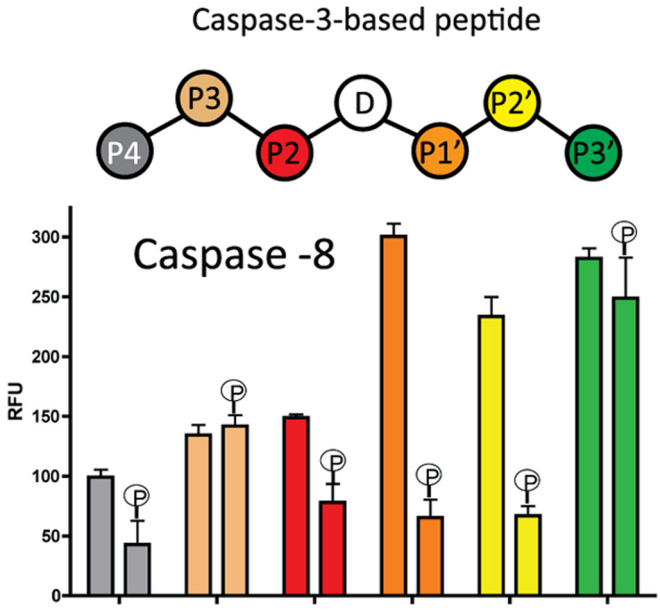

FIG. 6. **Relative activity of caspase-8 with model peptides containing serine or phosphoserine at each position from P4 to P3′.** Peptides modeled after the caspase-8 cleavage site of pro-caspase-3 were incubated with caspase-8 (100 nM) for 5 min at 37 °C before the reaction was terminated by an excess of the irreversible caspase inhibitor zVAD-fmk. Error bars represent the standard deviation of four reactions. Means of the caspase activities toward the phosphorylated and the corresponding nonphosphorylated peptide were compared using analysis of variance and Tukey's test. All pairs had p values < 0.001, except for the P3 and P3′ pair, which had p values > 0.05.

proteolysis of proteins. Importantly, our peptide cleavage assays revealed that phosphoserine within, or just proximal to, the canonical caspase consensus motif is primarily inhibitory. Taken together with the observation that MST3 proteolysis is promoted by phosphorylation, this supports a model by which substrate phosphorylation can promote caspase motif accessibility or structure when occurring outside of the context of the motif itself. One potential limitation of our approach relates to the high stoichiometry of caspase-site phosphorylation required in order for a difference in susceptibility to be measurable. In an effort to overcome this limitation, we treated cells with okadaic acid to preserve phosphosite occupancy. Similarly, the effect of phosphorylation on cleavage is not necessarily absolute, such as at P3′, for example. To avoid complete digestion of proteins with phosphorylation sites at these residues, we used two different caspase concentrations. Despite these caveats, we were able to uncover a number of modulated caspase substrates and validated Yap1, MST3, and Golgin-160 as caspase targets that experience altered degradation in response to lysate dephosphorylation.

Yap1 and Golgin-160 have phosphoacceptor residues at positions that, when occupied with phosphate, were inhibitory toward the cleavage of peptide substrates. Although the phosphorylation status of P4 serine on Golgin-160 and P1′ threonine on Yap1 has not been confirmed in phospho-proteomics studies, their occupancy would be consistent with cleavage patterns we observed on peptide substrates and in lysate cleavage assays. At this point, we cannot rule out that remote phosphorylation sites may contribute to reduced susceptibility to proteolysis in a manner similar to how phosphorylation at S422 on Acinus-S reduces cleavage at D355 (12). Interestingly, Golgin-160, like other members of the Golgi complex, is dismantled via caspase cleavage early in the apoptotic response (36). Golgin-160 is cleaved at D_{59}, D_{139}, and D_{311}—the site we identified—with purified caspases and in cells after treatment with diverse apoptotic stimuli (30). In our validation studies, we inferred via differential migration of Golgin-160 cleavage products that two sites (D_{59} and D_{139}) were cleaved in phosphorylated lysates but that proteolysis at $SEVD_{311}$ was blocked by phosphorylation. Interestingly, in response to apoptotic signals initiating from death receptors or endoplasmic reticulum stress, noncleavable forms of Golgin-160 can actually block apoptotic progression (31), though the effect of blocking each caspase site in isolation remains unknown. Yap1 is another caspase target that we validated for which phosphorylation inhibits caspase cleavage. $DEMD_{424}$ has not previously been identified as a caspase cleavage site, but $ASTD_{111}$ is cleaved in Jurkat cells in response to apoptotic induction by TRAIL and staurosporine, perhaps explaining why we observed multiple cleavage products in our validation studies (28). Furthermore, P3 and P2 of $ASTD_{111}$ have previously been identified as phosphorylated in cells (37), perhaps clarifying results from our Western blots that indicated multiple cleavage products were differentially regulated between the phosphorylated and phosphatase-treated lysates. In terms of functionality, Yap1 is a transcriptional effector of the MST1 and MST2 kinases (38), which are also targeted by caspases and function in apoptotic progression (24, 39). Interestingly, MST1 and MST2 contain previously identified phosphorylation sites at P1′ and P3′, suggesting that caspase cleavage of multiple constituents of the same pathway is hierarchically regulated by phosphorylation (40). As well, MST1 phosphorylation by Akt at T387, a site distant from the scissile bond, blocks cleavage (41), further implicating the control of proteolytic processing of this pathway as an important signaling event.

In the case of MST3, treating cells with the phosphatase inhibitor calyculin A promotes phosphorylation, activation, and structural reordering that alters its interaction partners (42). One interpretation of our data supports a model whereby MST3 is preferentially cleaved in its active form because our N-terminomic strategies used lysates from cells treated with okadaic acid, a phosphatase inhibitor that, like calyculin A, inhibits PP1 and PP2 (42). As well, MST3 is a pro-apoptotic kinase that exhibits increases in activity after the removal of its C terminus by caspase cleavage (29). A function of this hypothetical hierarchical layer of regulation is that phosphorylation and cleavage could provide graded levels of MST3 activity.

As a logical extension of the unbiased investigation of the effect of phosphorylation on caspase-mediated degradation in the proteome, we were also interested in systematically evaluating the determinant properties of phosphorylated residues in the context of model substrate peptides. Given the size and charge of phosphoryl residues, we speculated that phosphorylation might have effects outside of the canonical P4–P1′ caspase motif. Along these lines, even unmodified amino acids have exhibited determinant properties at P6, P5, P2′, and P3′, and Dix *et al.* (15) recently catalogued a large number of caspase sites with phosphorylated residues in an extended motif, though precise effects of phosphorylated residues at many positions remain unknown (34). In systematically analyzing the positional effect of phosphoserine on caspase cleavage, we found that phosphorylated residues outside the canonical caspase motif inhibited caspase-mediated cleavage. Prime side (C-terminal of the scissile bond) determinants inhibited cleavage as far away as four residues from the scissile bond, and the inhibitory capacity was inversely proportional to the distance from the catalytic machinery. This finding may be partly explained by previous observations made by Stennicke *et al.* (33), who showed that negative determinants at P1′ fail to stabilize the transition state, and therefore the bulky, highly charged phosphoserine might act similarly, but with diminishing effects when distanced from the catalytic machinery. There is also evidence of an S5 binding site (interacting with P5) on caspases in that P5 residues positively influence cleavage by caspase-3 (43) and direct selectivity between caspase-3 and caspase-7 (34). We investigated the effect of phosphorylation at this position, observing inhibitory effects consistent with a preference for small non-polar residues by caspase-3 (34). The determinant properties of P5 on caspase-7 are less obvious, making specific reasons for phospho-P5 difficult to reconcile (34). Interestingly, phosphoserine at P5 in the Golgin-160 series resulted in little change in cleavage, suggesting that the effects at this position might be context dependent.

Inhibitory effects at P4, P2, and P1′ were consistent with the literature, but we did note a discrepancy at the P3 position. Dix *et al.* (15) found that phosphorylated P3 on substrate peptides is strictly a positive factor for caspase-8 cleavage and either promotes or has no effect on caspase-3 mediated degradation, whereas, like Toszer *et al.* (8), we observed no effect at this site for both caspase-3 and caspase-8. We cannot definitively explain this discordance, but we can speculate that reaction conditions might have played a role. First, Dix *et al.* (15) used enzyme:substrate ratios 10-fold to 100-fold greater than our own, and reaction times that were 20 times longer, suggesting that their enzymes were less stable. For caspase-8, we used the chaotropic agent sodium citrate, which promotes caspase activity by stabilizing the dimeric form (44). Collectively, it is possible that determinant properties of phosphorylated P3 might depend on reaction conditions that affect enzyme stability. Another possibility is that the results were affected by the substrate peptides used; Dix and colleagues (15) tended toward longer peptides and those with sequences that differed from our model, suggesting that lengthier peptides or pairwise primary amino acid interactions could affect cleavage. At minimum, our mutual findings are consistent in that phosphorylated P3 did not universally inhibit cleavage.

In accordance with the literature, phospho-P2 and phospho-P1′ were also inhibitory toward proteolysis (8, 13). Of note was the measureable activity of caspase-8 against these peptides, whereas activity of caspase-3 and caspase-7 was not detected under the conditions used. Furthermore, baseline levels of cleavage by caspase-8 for peptides phosphorylated at P2′ and P4 were also above background, perhaps suggesting greater tolerance against inhibitory effects of caspase-8 site phosphorylation. Along these lines, the only known caspase-8 protein substrates negatively regulated by phosphorylation are phosphorylated at two sites within the cleavage motif; phosphorylation at P2 and P1′ of procaspase-3 blocks its cleavage by caspase-8 (13), and phosphorylated P2 and P2′ prevents cleavage of Bid (9). In this way, phosphorylation at multiple, slightly tolerated positions might function to grade cleavage and modulate signaling output.

In summary, we used two strategies to elucidate the interplay between caspase substrate phosphorylation and proteolysis. We systematically characterized the primary sequence determinant properties of phosphoserine within peptide substrates, and we also utilized an unbiased, N-terminomic approach to monitor caspase substrates that were regulated by phosphorylation in the context of the proteome. Overall, we anticipate that efforts such as ours that clarify the hierarchical regulation of caspase substrate phosphorylation and cleavage will improve our understanding of apoptotic signaling and the regulatory mechanisms that control cell survival.

Acknowledgments—We thank Dr. Sean Cregan for providing access to a fluorescent plate reader; Dr. Huadong Liu for help with peptide synthesis; and Nathan Cox, Dennis Goldfarb, Paula Pittock, Dr. Chris Hughes, and past and present members of the Litchfield laboratory for helpful discussions.

* J.P.T. was supported by a Doctoral Banting and Best Canada Graduate Scholarship and a Canada Graduate Scholarship Michael Smith Foreign Study Supplement. J.D.R.K. was supported by a postdoctoral fellowship from the Heart and Stroke foundation of Canada. S.A.Z. was supported by the CIHR Strategic Training Program in Cancer Research and Technology Transfer and an Ontario Graduate Scholarship. This work was funded by grants from the Canadian Institutes of Health Research (to D.W.L.), the National Sciences and Engineering Research Council (to G.A.L.), the Canadian Cancer Society (to S.S.L.), the National Institutes of Health (Grant No. GM101141), and the University Cancer Research Fund (UNC-CH) (to G.L.J. and L.M.G.). The UNC Michael Hooker Proteomics Center was supported by the NCI, National Institutes of Health (Grant No. CA016086).

S This article contains supplemental material.

REFERENCES

1. Cohen, G. M. (1997) Caspases: the executioners of apoptosis. *Biochem. J.* **326(Pt 1),** 1–16
2. Hanahan, D., and Weinberg, R. A. (2000) The hallmarks of cancer. *Cell* **100,** 57–70
3. Hunter, T. (2000) Signaling—2000 and beyond. *Cell* **100,** 113–127
4. Taylor, R. C., Cullen, S. P., and Martin, S. J. (2008) Apoptosis: controlled demolition at the cellular level. *Nat. Rev. Mol. Cell. Biol.* **9,** 231–241
5. Olsson, M., and Zhivotovsky, B. (2011) Caspases and cancer. *Cell Death Differ.* **18,** 1441–1449
6. Kurokawa, M., and Kornbluth, S. (2009) Caspases and kinases in a death grip. *Cell* **138,** 838–854
7. Duncan, J. S., Turowec, J. P., Vilk, G., Li, S. S., Gloor, G. B., and Litchfield, D. W. (2010) Regulation of cell proliferation and survival: convergence of protein kinases and caspases. *Biochim. Biophys. Acta* **1804,** 505–510
8. Tozser, J., Bagossi, P., Zahuczky, G., Specht, S. I., Majerova, E., and Copeland, T. D. (2003) Effect of caspase cleavage-site phosphorylation on proteolysis. *Biochem. J.* **372,** 137–143
9. Desagher, S., Osen-Sand, A., Montessuit, S., Magnenat, E., Vilbois, F., Hochmann, A., Journot, L., Antonsson, B., and Martinou, J. C. (2001) Phosphorylation of bid by casein kinases I and II regulates its cleavage by caspase 8. *Mol. Cell* **8,** 601–611
10. Walter, J., Schindzielorz, A., Grunberg, J., and Haass, C. (1999) Phosphorylation of presenilin-2 regulates its cleavage by caspases and retards progression of apoptosis. *Proc. Natl. Acad. Sci. U.S.A.* **96,** 1391–1396
11. Walter, J., Grunberg, J., Schindzielorz, A., and Haass, C. (1998) Proteolytic fragments of the Alzheimer's disease associated presenilins-1 and -2 are phosphorylated in vivo by distinct cellular mechanisms. *Biochemistry* **37,** 5961–5967
12. Hu, Y., Yao, J., Liu, Z., Liu, X., Fu, H., and Ye, K. (2005) Akt phosphorylates acinus and inhibits its proteolytic cleavage, preventing chromatin condensation. *EMBO J.* **24,** 3543–3554
13. Duncan, J. S., Turowec, J. P., Duncan, K. E., Vilk, G., Wu, C., Luscher, B., Li, S. S., Gloor, G. B., and Litchfield, D. W. (2011) A peptide-based target screen implicates the protein kinase CK2 in the global regulation of caspase signaling. *Sci. Signal.* **4,** ra30
14. Kleifeld, O., Doucet, A., auf dem Keller, U., Prudova, A., Schilling, O., Kainthan, R. K., Starr, A. E., Foster, L. J., Kizhakkedathu, J. N., and Overall, C. M. (2010) Isotopic labeling of terminal amines in complex samples identifies protein N-termini and protease cleavage products. *Nat. Biotechnol.* **28,** 281–288
15. Dix, M. M., Simon, G. M., Wang, C., Okerberg, E., Patricelli, M. P., and Cravatt, B. F. (2012) Functional interplay between caspase cleavage and phosphorylation sculpts the apoptotic proteome. *Cell* **150,** 426–440
16. Kleifeld, O., Doucet, A., Prudova, A., auf dem Keller, U., Gioia, M., Kizhakkedathu, J. N., and Overall, C. M. (2011) Identifying and quantifying proteolytic events and the natural N terminome by terminal amine isotopic labeling of substrates. *Nat. Protoc.* **6,** 1578–1611
17. Cox, J., and Mann, M. (2008) MaxQuant enables high peptide identification rates, individualized p.p.b.-range mass accuracies and proteome-wide protein quantification. *Nat. Biotechnol.* **26,** 1367–1372
18. Crooks, G. E., Hon, G., Chandonia, J. M., and Brenner, S. E. (2004) WebLogo: a sequence logo generator. *Genome Res.* **14,** 1188–1190
19. Gyenis, L., Duncan, J. S., Turowec, J. P., Bretner, M., and Litchfield, D. W. (2011) Unbiased functional proteomics strategy for protein kinase inhibitor validation and identification of bona fide protein kinase substrates: application to identification of EEF1D as a substrate for CK2. *J. Proteome Res.* **10,** 4887–4901
20. Zhou, Q., Snipas, S., Orth, K., Muzio, M., Dixit, V. M., and Salvesen, G. S. (1997) Target protease specificity of the viral serpin CrmA. Analysis of five caspases. *J. Biol. Chem.* **272,** 7797–7800
21. Denault, J. B., and Salvesen, G. S. (2003) Expression, purification, and characterization of caspases. *Curr. Protoc. Protein Sci.* Chapter 21, Unit 21.13
22. McStay, G. P., Salvesen, G. S., and Green, D. R. (2008) Overlapping cleavage motif selectivity of caspases: implications for analysis of apoptotic pathways. *Cell Death Differ.* **15,** 322–331
23. Thornberry, N. A., Rano, T. A., Peterson, E. P., Rasper, D. M., Timkey, T., Garcia-Calvo, M., Houtzager, V. M., Nordstrom, P. A., Roy, S., Vaillancourt, J. P., Chapman, K. T., and Nicholson, D. W. (1997) A combinatorial approach defines specificities of members of the caspase family and granzyme B. Functional relationships established for key mediators of apoptosis. *J. Biol. Chem.* **272,** 17907–17911
24. Graves, J. D., Gotoh, Y., Draves, K. E., Ambrose, D., Han, D. K., Wright, M., Chernoff, J., Clark, E. A., and Krebs, E. G. (1998) Caspase-mediated activation and induction of apoptosis by the mammalian Ste20-like kinase Mst1. *EMBO J.* **17,** 2224–2234
25. Emoto, Y., Manome, Y., Meinhardt, G., Kisaki, H., Kharbanda, S., Robertson, M., Ghayur, T., Wong, W. W., Kamen, R., and Weichselbaum, R. (1995) Proteolytic activation of protein kinase C delta by an ICE-like protease in apoptotic cells. *EMBO J.* **14,** 6148–6156
26. Agard, N. J., Mahrus, S., Trinidad, J. C., Lynn, A., Burlingame, A. L., and Wells, J. A. (2012) Global kinetic analysis of proteolysis via quantitative targeted proteomics. *Proc. Natl. Acad. Sci. U.S.A.* **109,** 1913–1918
27. Mahrus, S., Trinidad, J. C., Barkan, D. T., Sali, A., Burlingame, A. L., and Wells, J. A. (2008) Global sequencing of proteolytic cleavage sites in apoptosis by specific labeling of protein N termini. *Cell* **134,** 866–876
28. Crawford, E. D., Seaman, J. E., Agard, N., Hsu, G. W., Julien, O., Mahrus, S., Nguyen, H., Shimbo, K., Yoshihara, H. A., Zhuang, M., Chalkley, R. J., and Wells, J. A. (2012) The DegraBase: a database of proteolysis in healthy and apoptotic human cells. *Mol. Cell. Proteomics* **12,** 813–824
29. Huang, C. Y., Wu, Y. M., Hsu, C. Y., Lee, W. S., Lai, M. D., Lu, T. J., Huang, C. L., Leu, T. H., Shih, H. M., Fang, H. I., Robinson, D. R., Kung, H. J., and Yuan, C. J. (2002) Caspase activation of mammalian sterile 20-like kinase 3 (Mst3). Nuclear translocation and induction of apoptosis. *J. Biol. Chem.* **277,** 34367–34374
30. Mancini, M., Machamer, C. E., Roy, S., Nicholson, D. W., Thornberry, N. A., Casciola-Rosen, L. A., and Rosen, A. (2000) Caspase-2 is localized at the Golgi complex and cleaves golgin-160 during apoptosis. *J. Cell Biol.* **149,** 603–612
31. Maag, R. S., Mancini, M., Rosen, A., and Machamer, C. E. (2005) Caspase-resistant Golgin-160 disrupts apoptosis induced by secretory pathway stress and ligation of death receptors. *Mol. Biol. Cell* **16,** 3019–3027
32. Slee, E. A., Adrain, C., and Martin, S. J. (2001) Executioner caspase-3, -6, and -7 perform distinct, non-redundant roles during the demolition phase of apoptosis. *J. Biol. Chem.* **276,** 7320–7326
33. Stennicke, H. R., Renatus, M., Meldal, M., and Salvesen, G. S. (2000) Internally quenched fluorescent peptide substrates disclose the subsite preferences of human caspases 1, 3, 6, 7 and 8. *Biochem. J.* **350 Pt 2,** 563–568
34. Demon, D., Van Damme, P., Vanden Berghe, T., Deceuninck, A., Van Durme, J., Verspurten, J., Helsens, K., Impens, F., Wejda, M., Schymkowitz, J., Rousseau, F., Madder, A., Vandekerckhove, J., Declercq, W., Gevaert, K., and Vandenabeele, P. (2009) Proteome-wide substrate analysis indicates substrate exclusion as a mechanism to generate caspase-7 versus caspase-3 specificity. *Mol. Cell. Proteomics* **8,** 2700–2714
35. Fuentes-Prior, P., and Salvesen, G. S. (2004) The protein structures that shape caspase activity, specificity, activation and inhibition. *Biochem. J.* **384,** 201–232
36. Mukherjee, S., Chiu, R., Leung, S. M., and Shields, D. (2007) Fragmentation of the Golgi apparatus: an early apoptotic event independent of the cytoskeleton. *Traffic* **8,** 369–378
37. Gnad, F., Gunawardena, J., and Mann, M. (2011) PHOSIDA 2011: the posttranslational modification database. *Nucleic Acids Res.* **39,** D253–D260
38. Hong, W., and Guan, K. L. (2012) The YAP and TAZ transcription co-activators: key downstream effectors of the mammalian Hippo pathway. *Semin. Cell Dev. Biol.* **23,** 785–793
39. Lee, K. K., Ohyama, T., Yajima, N., Tsubuki, S., and Yonehara, S. (2001) MST, a physiological caspase substrate, highly sensitizes apoptosis both upstream and downstream of caspase activation. *J. Biol. Chem.* **276,** 19276–19285
40. Turowec, J. P., Duncan, J. S., Gloor, G. B., and Litchfield, D. W. (2011) Regulation of caspase pathways by protein kinase CK2: identification of proteins with overlapping CK2 and caspase consensus motifs. *Mol. Cell. Biochem.* **356,** 159–167
41. Jang, S. W., Yang, S. J., Srinivasan, S., and Ye, K. (2007) Akt phosphorylates MstI and prevents its proteolytic activation, blocking FOXO3 phosphorylation and nuclear translocation. *J. Biol. Chem.* **282,** 30836–30844
42. Fuller, S. J., McGuffin, L. J., Marshall, A. K., Giraldo, A., Pikkarainen, S.,

Clerk, A., and Sugden, P. H. (2012) A novel non-canonical mechanism of regulation of MST3 (mammalian Sterile20-related kinase 3). *Biochem. J.* **442,** 595–610
43. Fu, G., Chumanevich, A. A., Agniswamy, J., Fang, B., Harrison, R. W., and Weber, I. T. (2008) Structural basis for executioner caspase recognition of P5 position in substrates. *Apoptosis* **13,** 1291–1302
44. Boatright, K. M., Renatus, M., Scott, F. L., Sperandio, S., Shin, H., Pedersen, I. M., Ricci, J. E., Edris, W. A., Sutherlin, D. P., Green, D. R., and Salvesen, G. S. (2003) A unified model for apical caspase activation. *Mol. Cell* **11,** 529–541
45. Mi, H., Muruganujan, A., Casagrande, J. T., and Thomas, P. D. (2013) Large-scale gene function analysis with the PANTHER classification system. *Nat. Protoc.* **8,** 1551–1566
46. Mi, H., Muruganujan, A., and Thomas, P. D. (2013) PANTHER in 2013: modeling the evolution of gene function, and other gene attributes, in the context of phylogenetic trees. *Nucleic Acids Res.* **41,** D377–D386